Powder Technology 336 (2018) 220–229

Contents lists available at ScienceDirect

Powder Technology

journal homepage: www.elsevier.com/locate/powtec

The onset of shock-induced particle jetting

Kun Xue [a,*], Haoran Cui [a], Kaiyuan Du [a], Xiaoliang Shi [a], Yixiang Gan [b], Chunhua Bai [a]

[a] State Key Laboratory of Explosive Science and Technology, Beijing Institute of Technology, Beijing 100081, China
[b] School of Civil Engineering, The University of Sydney, Sydney, Australia

ARTICLE INFO

Article history:
Received 27 September 2017
Received in revised form 9 April 2018
Accepted 24 May 2018
Available online 26 May 2018

Keywords:
Particle jetting
Dynamic jamming front
Unjamming
Discrete element method
Hele-Shaw cell
Pattern formation

ABSTRACT

The shock dispersal of particle shells or rings by radially divergent impulsive loads takes the form of coherent particle jets which have much larger dimensions from those associated with the constituent grains. In the present study, quasi-two-dimensional particle jetting is studied via both experiments based on a radial Hele-Shaw cell and numerical simulations using the discrete element method. Simulations agree well with the experiments in terms of the branched jet pattern and characteristic timescale for jet growth. Besides simulations reproduce the signature events defining the jet formation observed in experiments, specifically the initiation of incipient jets from the non-perturbed internal surface of ring, as well as the concurrent ramification and annihilation of jets. More importantly the particle-scale simulations reveal the physics underlying the jet inception. We found that the onset of particle jetting corresponds to the transition of the shock jammed band which homogeneously expands outwards to the unevenly spaced localized shear flows, or equivalently, unjamming of the dynamic jamming front.

1. Introduction

Particle jetting during the explosive or shock dispersal of particles has been widely observed in nature and many military applications, such as volcanic eruption, explosion of landmines, thermobaric explosion, high-speed intruder striking granular media, and particle jets impacting targets, etc. [1–9]. A typical configuration involves particle rings or shells being exposed to radially divergent blast or shock fronts [1–8]. The resulting expanding cloud of explosion or shock disseminated materials comprises of large particle agglomerates which protrude to finger- or spike-like particle jets. Predicting the jet number has been an active area of research which requires the fundamental understanding of the physics underlying the jet formation [3,4,6–8,10].

Several theories have been put forward to account for the explosion driven particle jetting, including the Richtmyer-Meshkov instability [10], brittle fracture mechanism [7] and dual particle jetting mechanism [11]. Whereas no consensus has been reached yet. Compared with the extensive investigations into the explosion driven particle jetting, there are quite limited efforts put into studying the particle jetting induced by moderate shock waves with a peak overpressure on the order of $O(10^4–10^6)$Pa [4,8,12,13]. Although both cases feature the resembling jetting pattern, we argue that the two jetting instabilities occur in different time scales and more importantly are governed by fundamentally different mechanisms since shock consolidation of particles which dominates the blast-particle interactions is negligible under weak shock loadings [13].

In the opposite extreme scenario, similar finger-like patterns are formed when particles are displaced by the gases, fluids and other particles in a quasi-static manner [14–17]. Specifically, Sandnes et al. present a unified description of emerging morphologies in granular mixtures injected by gases in the form of extended phase diagrams [15]. During the viscous regime the hydrodynamic interactions dominate at high flow rate. Viscous granular fingers result from the competition between the viscous fluid drag and the friction between grains and against the confinement [14,15]. Again this theory doesn't hold for the shock induced particle jetting since in the latter case the build-up of friction is absent due to the overwhelming inertial forces and the hydrodynamic interactions play a minor role in the shock interaction regime.

Combining the radial Hele-Shaw cell which is commonly used in studying the particle fingering and the shock tube, Rodriguez et al. investigated the formation of particle jetting in a quasi-two-dimensional configuration and derived empirical relations between the jet number and a variety of structural parameters [4,8]. The experimental work done by Rodriguez et al. is more focused on the well-developed jet structure after the jets penetrate the external surface of ring [4,8]. Our previous simulations based on the discrete element method (DEM) performed instead reveal particle scale dynamics of jet formation before the penetration using similar configurations [13]. We argue that the heterogeneous network of force chains formed in the shock compacted particles is responsible for the formation of fast- and slow-moving particle clusters around the internal perimeter observed

* Corresponding author.
E-mail address: xuekun@bit.edu.cn (K. Xue).

https://doi.org/10.1016/j.powtec.2018.05.056
0032-5910/

in experiments [4]. But the intricate interplay between the erratic force structure and the flow patterns is far from clear thanks to the constant destruction and re-construction of the network of force chains as a result of ever-changing particle packing.

The aim of the present work is to elaborate the physics defining the inception of shock-induced jets from the particle-scale perspective. To this end, the particle scale information regarding the evolution of particle contact forces and velocities is necessary, which can be accessed by DEM simulations. Experiments based on the same quasi-two-dimensional configuration were also carried out to validate the simulation results.

2. Numerical and experimental setup

Originally developed by Cundall and Strack [18], the DEM is a numerical scheme that has been successfully used to simulate the response of granular media by modeling the dynamic behavior of large assemblies of circular disks, spheres, and blocks [9,13,19–22]. The motion of each particle in the assembly is governed by the following equations

$$\begin{cases} m_i \dfrac{\mathrm{d}V_i}{\mathrm{d}t} = \displaystyle\sum_{j=1}^{n_i^c} F_{ij}^c + F_i^g + F_i^{ex} \\ I_i \dfrac{\mathrm{d}\omega_i}{\mathrm{d}t} = \displaystyle\sum_{j=1}^{n_i^c} M_{ij} \end{cases} \tag{1}$$

where V_i and ω_i denote the translational and angular velocities of particle i, respectively; F_{ij}^c and M_{ij} are the contact force and contact torque acting on particle i by particle j or the wall(s), respectively; n_i^c is the number of total contacts for particle i; F_i^g is the gravitational force, and F_i^{ex} is other external force; m_i and I_i are the mass and moment of inertia of particle i. The Hertz-Mindlin contact law is employed in conjunction with Coulomb's friction law to describe the inter-particle contact behavior. Details of the contact model and the parameters used in the simulations are presented in Appendix I.

The particle packing is established by first letting free-falling spherical quartz sand particles settle by gravity in annular simulation boxes and allowing them to relax until the kinetic energy of assembly ceases to decrease. A series of particle rings were generated this way with the inner diameter normalized by the particle diameter, $\hat{D}_{in} = D_{in}/d_p$, ranging from 200 to 1600. The normalized width of ring, $\hat{w} = (D_{out} - D_{in})/(2d_p)$, was kept constant, $\hat{w} = 400$. The resulting short annular particle bands have the height 2–3 times the particle diameter. The friction between container walls (i.e., the top and bottom plates) and grains is negligible. Thus the three-dimensional effect becomes negligible.

In the present simulations, the shock loading is achieved by applying constant forces on particles residing along the internal perimeter as shown in Fig. 1. The magnitude of the force applied on each particle equals to the cross-section area of this particle multiplied by the overpressure, Δp_0, which ranges from 0.5 to 10 bar. Also the applied force vector aligns with the local radial direction. Ref [4] compares the effects of overpressure profiles on the jet pattern and found no noticeable differences in patterns generated by the pressure jumps followed by a constant value or a rapid decline. A specific loading algorithm was invoked to mimic the penetration of pressurized gases trapped inside the particle ring into the bulk, which is manifested by particles clustering around the cusps of the disturbed internal surface persistently being subjected to the impulsive loads (see Fig. 1(b)). Details of the loading algorithm can be referred to Ref [13].

In order to verify the numerical results, we also performed experiments of the shock dispersion of the quartz sand ring using moderate shock waves. The quasi-two-dimensional configuration setup as schematized in Fig. 2 consists of a radial Hele-Shaw cell and a vertical shock tube similar to that used in Refs. [4, 8, 12]. The outlet of the shock tube is fitted vertically beneath the Hele-Shaw cell, matching the hole in the bottom plate with the same diameter. A concentric particle ring disposed around the bottom hole consisting of fine quartz grains with the average diameter of 50 μm is trapped between the top and bottom plates of the Hele-Shaw cell. The incident shock wave and the trailing pressurized gas flows bursting out of the shock tube hit the top plate and are forced through the gap between the top and

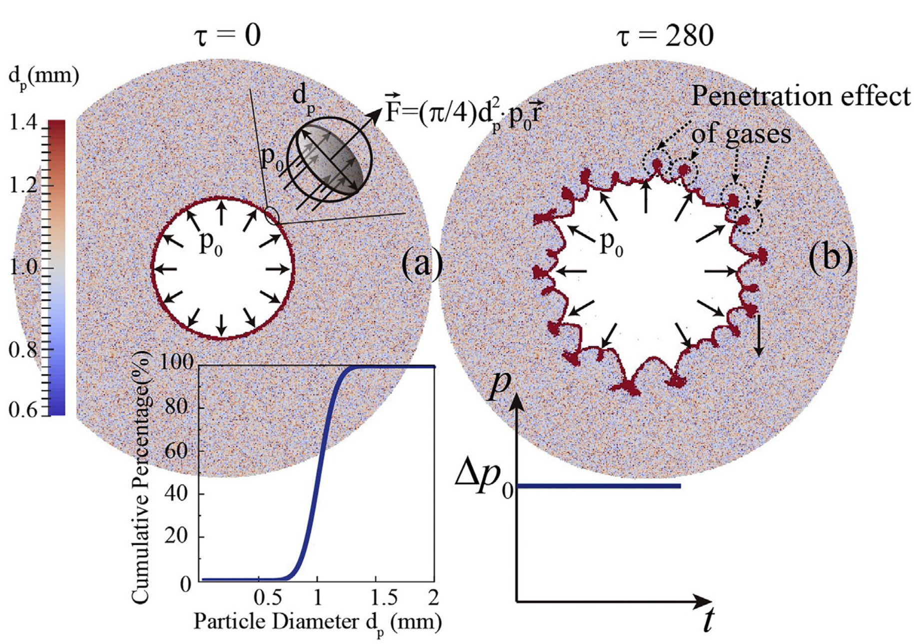

Fig. 1. Snapshots (top views) of the particle ring ($\hat{D}_{in} = 400$) before (a) and after (b) the loading. Particles in the innermost layers and clustering around the cusps of the internal surface (shaded red) are subjected to the radially directed constant forces which are proportional with the cross-section areas of the individual particles. The proportional factor is the peak overpressure Δp_0. Insets of (a) and (b) represent the statistical distribution of particle diameter, d_p, and the profile of the impulsive load used in the simulations. (For interpretation of the references to colour in this figure legend, the reader is referred to the web version of this article.)